Optical Label Swapping Using Payload Envelope Detection Circuits

Zhaoyang Hu, *Member, IEEE*, Roopesh Doshi, Hsu-Feng Chou, Henrik N. Poulsen, David Wolfson, John E. Bowers, *Fellow, IEEE*, and Daniel J. Blumenthal, *Fellow, IEEE*

***Abstract*—Optical label swapping of 10-Gb/s nonreturn-to-zero (NRZ) labels attached to 40-Gb/s return-to-zero payloads is demonstrated using payload envelope detection (PED) circuits based on 40-Gb/s clock recovery with nanosecond locking time. The circuits generate a digital envelope signal representing the payload location without having to process the 40-Gb/s data. The low-frequency PED signal, which is generated from the recovered 40-GHz packet clock by a radio-frequency mixer, can be utilized to erase/rewrite the label through traveling-wave electroabsorption modulators. This approach does not require active timing control to erase the label. Nearly penalty-free rewriting of a new 10-Gb/s NRZ label was demonstrated.**

***Index Terms*—Clock recovery (CR), label swapping, optical label swapping network, packet switching.**

I. Introduction

OPTICAL label swapping is required to enable networks to scale to a large number of nodes and high capacity [1]–[3]. Label swapping involves detection, erasure, and rewriting of the optical label without passing the payload through the electronic domain. In the approach addressed in this letter, the label is serially located in front of the payload and can be encoded at a lower bit rate and different modulation formats from the payload [1], [4], [5]. A key issue is that electronic processing of label data must be synchronized with t the location of the optical payload in order to erase the label. Knowing the location of the payload without processing the bits in the payload is, therefore, a key function that needs to be realized and implemented.

In this letter, we describe a new technique called payload envelope detection (PED) to erase and rewrite optical labels, which is used to identify the payload location in time with high temporal accuracy without processing the bits inside the payload. This approach uses the frequency discriminating feature of the clock recovery (CR) to detect the envelope of 40-Gb/s return-to-zero (RZ) payloads from the incoming packets. In the PED circuit, a 40-GHz clock is first recovered from the 40-Gb/s optical RZ payloads through the CR based on the techniques of filtering and threshold decision. The recovered 40-GHz payload clock is split and self-mixed to obtain the low-frequency sideband, i.e., the PED signal. We measured the characteristics of the PED signal, including dynamic range, flatness, root-mean-square (rms) jitter, and locking time against the input optical packet power. The PED circuit uses fast electrical processing, and no extra delay is required when gating a traveling-wave electroabsorption modulator (TW-EAM) for label erasure. Details of the low driving voltage TW-EAM have previously been reported in [7]. A new label can then be inserted by using the PED signal to gate another TW-EAM. The recovered 40-GHz clock can also be used for the receiver or regenerator depending on the applications.

Manuscript received February 8, 2005; revised March 19, 2005. This work was supported by the Defense Advanced Research Projects Agency (DARPA)/MTO DOD-N program under the LASOR project award number W911NF-04-9-0001.

The authors are with the Department of Electrical and Computer Engineering, Universtiy of California, Santa Barbara, CA 93106-9560 USA (e-mail: huby@ece.ucsb.edu).

Digital Object Identifier 10.1109/LPT.2005.848541

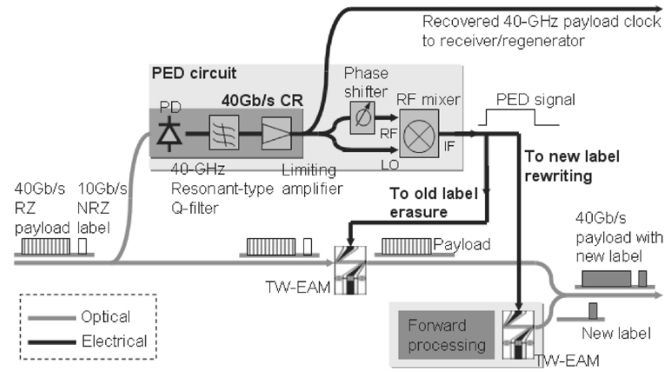

Fig. 1. Scheme of label erasure/rewriting using PED circuits.

II. Payload Envelope Detection

The basic circuit arrangement for PED is shown in Fig. 1. We use optical packets that consist of 40-Gb/s variable length RZ payloads and serial 10-Gb/s nonreturn-to-zero (NRZ) labels. The labels have no 10- or 40-GHz clock tones. The PED signal can be extracted by using a CR that only recovers the payload clock and a subsequent frequency mixing circuit. The 40-Gb/s CR is made of a photodetector (PD) with 40-GHz bandwidth, a resonant-type Q-filter with Q-factor of 800 at the center frequency of 39.8 GHz, and a limiting amplifier with 40-dB small signal gain. The recovered packet clock from the CR can be described as a frequency modulated signal

$$V(t) = \cos(\omega_0 t) V_{\text{Env}}(\omega_1 t) \quad (1)$$

where ω_0 and ω_1 are the frequencies of the carrier (the clock of the payload) and the sidebands (the envelop signal of the payload), respectively; $V_{\text{Env}}(\omega_1 t)$ is PED signal, which has the form of the square wave

$$V_{\text{Env}}(\omega_1 t) = \sum_{m=1} \left(1 + \frac{1}{2m-1} \cos((2m-1)\omega_1 t)\right). \quad (2)$$

In order to detect the PED signal, the recovered packet clock is split and then one part goes to the local oscillator port of

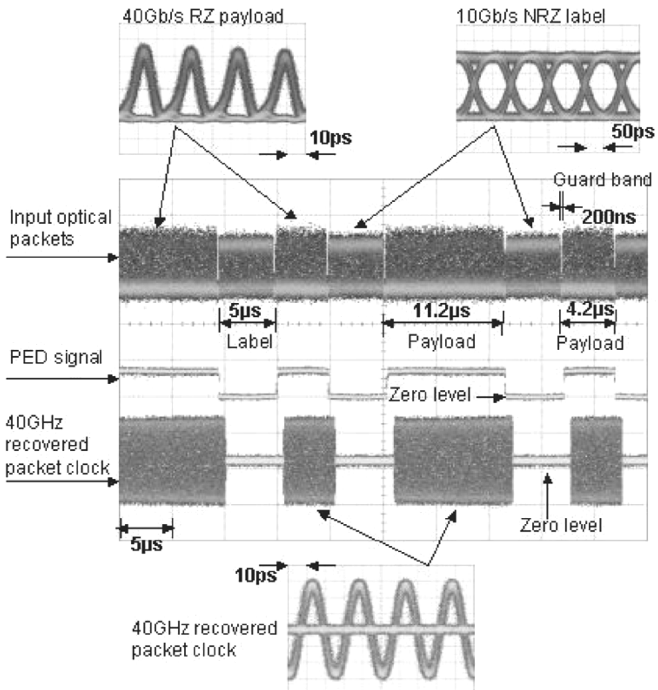

Fig. 2. Oscilloscope traces of the recovered 40-GHz packet clock (lower), the PED signal (middle) detected from the input optical packets (upper). Inset: Corresponding eye diagrams.

a radio-frequency (RF) mixer, and the other part goes to the RF port after a phase shifter with phase change ϕ at the carrier frequency. The low-frequency IF signal from the RF mixer, i.e., the PED signal, can be simplified as

$$\mathrm{PED}(\omega_1 t) = A\cos(\phi)V_{\mathrm{Env}}^2(\omega_1 t) \tag{3}$$

assuming that the phase delay is negligible at the payload envelop frequency. From (3), we can observe that the phase change ϕ can change the amplitude and sign of the PED signal. The shape of the detected envelope is proportional to the square of the original envelope, which makes no significant impact because the envelope signal is a square wave function.

In the experiment, a 10-GHz mode-locked fiber ring laser was used to generate RZ pulses at 1556 nm which were subsequently modulated with a $2^{31}-1$ pseudorandom binary sequence (PRBS) pattern through a $LiNbO_3$ modulator. Then optical 40-Gb/s RZ payloads were generated by gating an acoustooptical modulator (AOM) after an optical 10–40 multiplexer. Optical 10-Gb/s NRZ labels were generated by another AOM which gates an NRZ signal. The NRZ signal is generated from a continuous-wave light source with 1556-nm wavelength modulated with $2^{31}-1$ PRBS pattern generated by another $LiNbO_3$ modulator. The input optical packet has two different payload lengths, 11.2 and 4.2 μs, both separated with a 5-μs-long label. Considering the 100-ns rise/fall time of the AOM and also the gating requirements of the bit-error-rate tester (BERT), guard bands between the payloads and the labels were set to 200 ns.

Fig. 2 depicts the input optical packet, the measured PED signal, and the recovered packet clock. Corresponding eye diagrams of the 40-Gb/s RZ payloads and 10-Gb/s NRZ labels are shown as inset waveforms at the top of Fig. 2. By adjusting the phase shifter in the PED circuit, the PED signal level is maximized and the corresponding PED signal is shown as the middle waveform in Fig. 2. The high level of the PED signal corresponds to the payload and the zero level corresponds to the label, respectively. The PED signal can be used to gate a TW-EAM to erase the label through appropriately reverse biasing the TW-EAM: The high level part of the PED signal swings the payloads to the transparent region of the TW-EAM, which allows the payloads go through, while the zero level part of the PED signal remains the labels at the absorption region of the TW-EAM, which suppresses the labels. The inserted waveform at the bottom of Fig. 2 is the 40-GHz recovered packet clock and its eye diagram. Less than 1-ps rms timing jitter of the recovered 40-GHz packet clock is measured by using the histogram mode of the sampling oscilloscope with 65-GHz electrical bandwidth.

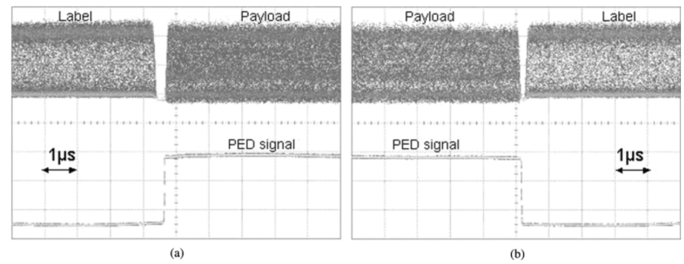

Fig. 3. Zoom in (a) front and (b) rear waveforms of input 40-Gb/s payload and recovered 40-GHz packet clock.

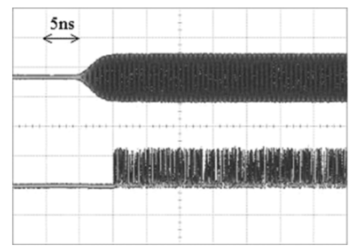

Fig. 4. Oscilloscope traces of the input 40-Gb/s payload (lower) and the recovered 40-GHz packet clock (upper).

We zoom in the front and rear parts of both the payloads and the corresponding PED signals, shown as the upper and lower waveforms in Fig. 3, respectively. It shows that the high-level window size of the PED signal is a little bit larger than the payloads due to the threshold effect in the PED circuits. Considering 200-ns-long guard bands, the PED signal is good enough to be used to erase and rewrite the labels. In the experiment, no extra delay is used to align the PED signal and the input optical packets partly due to the high-level window size and partly due to as fast as nanosecond-order processing time of the PED circuits.

In order to evaluate the locking time of the 40-Gb/s CR, we used a 40-Gb/s BERT to generate optical payloads with fixed pattern of 1 011 000 011 001 010…, shown as the lower waveform in Fig. 4. The corresponding recovered packet clock from the 40-Gb/s CR is shown as the upper waveform in Fig. 4. It shows that the 40-Gb/s CR recovers the clock within 5 ns.

III. Label Swapping Experiment

We measured the characteristics of the PED signal, shown in Fig. 5. The PED signal level increases monotonously when

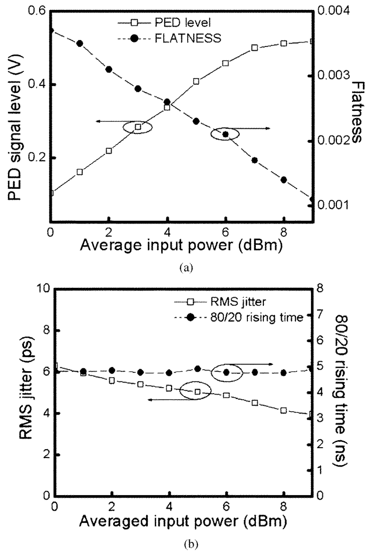

Fig. 5. (a) PED signal level and its flatness and (b) rms jitter and 80/20 rising time of the PED signal against the input average packet power.

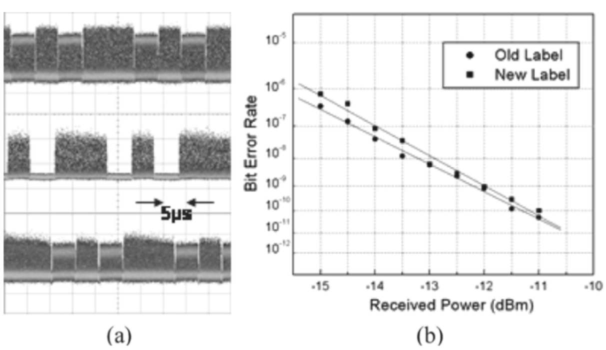

Fig. 6. (a) Demonstration of label swapping: waveforms of old label erasure (middle) and new label rewriting (lower) from the input optical packets (upper). (b) Measured BER results of label erasure and rewriting.

increasing the average power of the input optical packets, shown as the solid curve in Fig. 5(a). Flatness of the PED signal is defined as the ratio of the fluctuation of the high level to the average value of the PED's high level. It is less than 0.4% in the range from 0- to 9-dBm input power, shown as the dashed curve in Fig. 5(a). The rms jitter of the PED signal is measured as the standard deviation of its rising edge using the histogram mode of the oscilloscope. When increasing the input power from 0 to 9 dBm, the rms jitter is reduced from 6.2 to 4 ps, shown as the solid curve in Fig. 5(b). For the input power range of 0 to 9 dBm, the 80/20 rising time of the PED signal is measured to be 5 ns also using the sampling oscilloscope, shown as the dashed curve in Fig. 5(b).

The TW-EAM used in the experiment has an extinction ratio of above 30 dB for the transverse-magnetic mode. The PED signal is amplified to be above 1.2 V in order to achieve above 30-dB extinction ratio of label erasure. Fig. 6(a) depicts the oscilloscope traces of input optical packets, and the packets after label erasure and label rewriting. When adjusting the reverse bias of the TW-EAM to 1.5 V, excellent label suppression was seen and evaluated to be 30 dB, shown as the middle waveform in Fig. 6(a) (after erbium-doped fiber amplifier (EDFA) amplification). Compared with the input 40-Gb/s payloads, the output payloads have the spiking in the front due to the dynamics of the EDFA. It can be solved through reducing the size of the labels to several hundred nanoseconds. To simplify the experiment, an AOM was used instead of another TW-EAM to generate the new labels inserted in front of the payloads. The lower waveform in Fig. 6(a) shows the optical packets with new labels.

The bit-error rate (BER) was measured for the original and rewritten label data, shown in Fig. 6(b). The power levels of the original and rewritten labels were adjusted to be almost equal. Error-free operation and less than 0.2-dB power penalty were obtained, shown in the BER plots in Fig. 6(b). Considering above 30-dB extinction ratio of the label erasure, the small difference in sensitivity of 0.2 dB could be due to minor differences in the label power levels with the same average input packet power.

IV. Conclusion

Ten-gigabit/second NRZ label swapping is demonstrated by utilizing the PED signal obtained from the 40-Gb/s RZ payloads. The PED signal has good flatness, fast turn on time, and low timing jitter based on a 40-Gb/s CR with nanosecond-order locking time. Above 30-dB label erasure extinction ratio is obtained using the PED signal to gate a TW-EAM. Compared to the other approaches that require much smaller label level so as to well erase the time-domain labels [4], [5], the approach using the PED does not have such constraint. To insert a new label, coarse timing control would be necessary to align the new label to the 40-Gb/s payloads. But no extra delay is necessary to align the PED signal for erasing the labels. It is promising for the optical label swapping with chip-level integration.

References

[1] D. J. Blumenthal, B. E. Olsson, G. Rossi, T. E. Dimmick, L. Rau, M. Masanovic, O. Lavrova, R. Doshi, O. Jerphagnon, J. E. Bowers, V. Kaman, L. A. Coldren, and J. Barton, "All-optical label swapping networks and technologies," *J. Lightw. Technol.*, vol. 18, no. 12, pp. 2058–2075, Dec. 2000.

[2] A. Carena, M. D. Vaughn, R. Gaudino, M. Shell, and D. J. Blumenthal, "OPERA: An optical packet experimental routing architecture with label swapping capability," *J. Lightw. Technol.*, vol. 16, no. 12, pp. 2135–2145, Dec. 1998.

[3] A. Viswanathan, N. Feldman, Z. Wang, and R. Callon, "Evolution of multiprotocol label switching," *IEEE Commun. Mag.*, vol. 36, no. 5, pp. 165–173, May 1998.

[4] P. Öhlén, B. E. Olsson, and D. J. Blumenthal, "All-optical header erasure and penalty-free rewriting in a fiber-based high-speed wavelength converter," *IEEE Photon. Technol. Lett.*, vol. 12, no. 6, pp. 663–665, Jun. 2000.

[5] B. E. Olsson, P. Ohlen, L. Rau, G. Rossi, O. Jerphagnon, R. Doshi, D. S. Humphries, D. J. Blumenthal, V. Kaman, and J. E. Bowers, "Wavelength routing of 40 Gbit/s packets with 2.5 Gbit/s header erasure/rewriting using an all-fiber wavelength converter," *Electron. Lett.*, vol. , 36, pp. 345–347, 2000.

[6] D. J. Blumenthal, A. Carena, L. Rau, V. Curri, and S. Humphries, "All-optical label swapping with wavelength conversion for WDM-IP networks with subcarrier multiplexed addressing," *IEEE Photon. Technol. Lett.*, vol. 11, no. 11, pp. 1497–1499, Nov. 1999.

[7] Y.-J. Chiu, H.-F. Chou, V. Kaman, P. Abraham, and J. E. Bowers, "High extinction ratio and saturation power traveling-wave electroabsorption modulator," *IEEE Photon. Technol. Lett.*, vol. 14, no. 6, pp. 792–794, Jun. 2002.